should be treated as quantum-mechanical operators. This implies, for example, that $I_z(t)$ and $I_z(t+t')$ in (26) are operators that in general do not commute, so that the correlation function must be redefined in terms of a symmetrized product $\frac{1}{2}[\overline{I_z(t)I_z(t+t')} + \overline{I_z(t+t')I_z(t)}]$. The last two references both show that such a redefinition does lead in the quantum limit to a corrected Nyquist formula in which $k_B T$ is replaced by (37). For a basic discussion of noise and quantum mechanics, the reader is also referred to Chap. 6 of the monograph by Robinson.[7]

IX. CONCLUSIONS

Beginning with the appropriate model of a Fermi–Dirac conduction-electron gas, we have derived the Johnson–Nyquist expression for thermal noise inside a metal. This noise is seen to originate in spontaneous fluctuations of current that occur when electrons are scattered from occupied momentum states near the surface of the Fermi sphere into unoccupied momentum states that are also near the surface of the Fermi sphere. The unlikely circumstance that Fermi–Dirac and Maxwell–Boltzmann statistics should both lead to the Johnson–Nyquist formula turns out to be a consequence of the fact that all of the charged particles are allowed to participate in the Maxwell–Boltzmann picture, while in the Fermi–Dirac picture only those electrons that are close to the Fermi surface are allowed to participate. An externally applied Ohm's law transport current was shown *not* to affect the level of thermal noise.

[1] J. B. Johnson, "Thermal agitation of electricity in conductors," Phys. Rev. **32**, 97–109 (1928).
[2] H. Nyquist, "Thermal agitation of electric charge in conductors," Phys. Rev. **32**, 110–113 (1928).
[3] A. van der Ziel, *Noise in Solid State Devices and Circuits* (Wiley, New York, 1986), Chap. 5.
[4] D. A. Bell, *Noise in the Solid State* (Wiley, New York, 1985), Chap. 1.
[5] C. Kittel, *Elementary Statistical Physics* (Wiley, New York, 1958), p. 141.
[6] C. Kittel and H. Kroemer, *Thermal Physics* (Freeman, New York, 1980), 2nd ed., p. 98.
[7] F. N. H. Robinson, *Noise and Fluctuation in Electronic Devices and Circuits* (Clarendon, Oxford, 1974).
[8] M. B. Weissman, "1/*f* noise and other slow, non-exponential kinetics in condensed matter," Rev. Mod. Phys. **60**, 537–571 (1988).
[9] P. Dutta and P. M. Horn, "Low-frequency fluctuations in solids: 1/*f* noise," Rev. Mod. Phys. **53**, 497–516 (1981).
[10] A. Ambrozy, *Electronic Noise* (McGraw-Hill, New York, 1982).
[11] C. J. Bakker and G. Heller, "On the Brownian motion in electrical resistance," Physica **6**, 262–274 (1939).
[12] C. Kittel, *Introduction to Solid State Physics* (Wiley, New York, 1986), 6th ed.
[13] D. K. C. MacDonald, *Noise and Fluctuations* (Wiley, New York, 1962), p. 48.
[14] H. B. Callen and T. A. Welton, "Irreversibility and generalized noise," Phys. Rev. **83**, 34–40 (1951).
[15] R. Kubo, "The fluctuation-dissipation theorem," Rep. Prog. Phys. **29**, 255–284 (1966).
[16] W. Jones and N. H. March, *Theoretical Solid State Physics* (Wiley–Interscience, New York, 1973), Vol. 2, pp. 754ff.
[17] L. D. Landau and E. M. Lifshitz, *Statistical Physics* (Addison-Wesley, Reading, MA, 1958), pp. 398ff, Vol. 5 of *Course of Theoretical Physics.*

Measurements of the transient motion of a simple nonlinear system

Archana Ojha, Stephen Moon, Barbara Hoeling, and P. B. Siegel
Physics Department, California State Polytechnic University, Pomona, California 91768

(Received 25 July 1990; accepted for publication 31 October 1990)

A freely rotating magnet placed above a solenoid and between a set of Helmholtz coils is used to examine properties of a nonlinear system. Accurate measurements of the angular velocity are made with a photogate timing device. The period-doubling route to chaos, multiple periodicities, and the behavior of transient motion are observed and measured.

I. INTRODUCTION

In the past 15 years, the field of nonlinear dynamics and chaos has grown tremendously. These topics are now starting to be covered in the undergraduate curriculum. Some properties of nonlinear systems are treated in courses in classical mechanics, and simple quantitative exercises and analyses are making their way into classes on computational physics.[1] Along with these classroom discussions on nonlinear systems, various experiments are being introduced into student laboratories.[2] The purpose of this article is to describe a simple, inexpensive apparatus, suitable for the undergraduate laboratory, which is rich in applications to the study of nonlinear systems.

The apparatus consists of a freely rotating compass needle placed above a solenoid and between a set of Helmholtz coils. The solenoid supplies a constant vertical magnetic field, while the Helmholtz coils are used to drive the system with an alternating magnetic field. With the help of a photogate timing device, the angular velocity of the compass needle is measured for a fixed angle.

A similar system without the vertical magnetic field has been studied by several authors.[3–5] In these experiments, data were taken with a pickup coil and a stroboscope. Very interesting results were obtained in displaying strange attractors,[4,5] period doubling,[3,4] and higher multiplicities.[3,4] In our setup, we use a photogate which allows a simple and accurate measurement of the time evolution of the system. The time dependence of transient states and the system's response to a perturbation, as well as period doubling and

higher periodicities, can be easily observed. In addition, all the equipment used in the experiment is inexpensive, and, in our case, was all found in our stockroom.

II. EXPERIMENTAL SETUP

The experimental setup is shown in Fig. 1. The complete apparatus was put together from other undergraduate experiments and demonstrations.

The magnet and stand is a CENCO (catalog number 78425) magnet, which is designed to measure the declination of the Earth's magnetic field. A magnet with a large magnetic moment-to-mass ratio mounted with minimal bearing friction is desirable. The CENCO magnet proved satisfactory and it is wide enough to be used with a photogate time device.

The Helmholtz coils belong to a standard experiment to measure the electron's charge-to-mass ratio. The particular brand used in our case was Uchida Yoko Model TG-13. The Helmholtz current is supplied by a function generator from Pasco (Student Function Generator PI-9598). This function generator is capable of producing a sufficiently large voltage to drive the compass at a low frequency, which, in our case, was 1.5 Hz. The voltage across the Helmholtz coils was measured on a digital oscilloscope.

A constant magnetic field, which can be oriented at any angle with respect to the Helmholtz field, is produced by a solenoid. The current through the solenoid is measured with a digital ammeter.

To measure the angular velocity of the magnet, a photogate timer was used and connected to an Apple IIe computer via a game port interface (Pasco AI-6575). The photogate timer measures the time the gate is blocked by the magnet. We refer to this quantity as the blocking time, which is inversely proportional to the angular velocity.

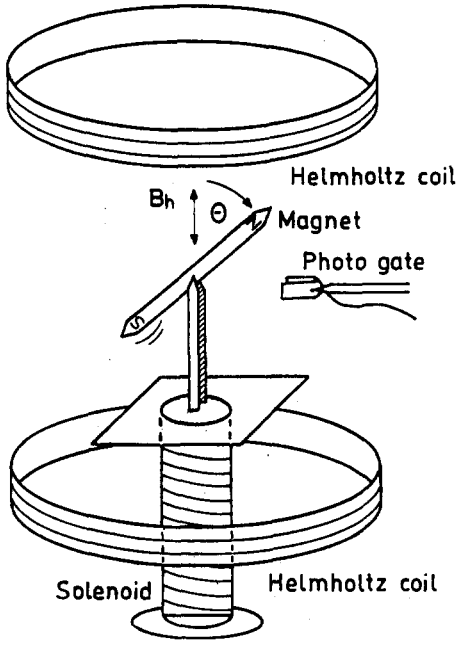

Fig. 1. A schematic of the experimental setup is shown. The spinning magnet is placed above a solenoid and between a pair of Helmholtz coils. The current in the solenoid is direct current, producing a constant vertical magnetic field. The current in the Helmholtz coils is sinusoidal and drives the magnet. Two different orientations of the Helmholtz coils, vertical and horizontal, were used.

Data were collected and analyzed with the assistance of "precision timer III" software from Vernier. The photogate was placed such that it recorded the blocking time when the magnet was around 20° from the vertical. The software allowed every other pass to be recorded, so we were able to measure successive blocking times after the magnet went through 360° of rotation.

There are three experimental quantities that are measured for a fixed frequency of the driving voltage in the coils: the peak-to-peak voltage across the Helmholtz coils, the current through the solenoid, and the blocking time of the spinning magnet at a particular angle. As will be shown, the blocking time can be measured to an accuracy of 0.5%, the current through the solenoid to within 1%, and the voltage across the coils to the resolution of the oscilloscope. This accuracy is sufficient to obtain very interesting results about the nonlinear system.

III. RESULTS

We have examined the response of the system for two different orientations of the constant magnetic field: perpendicular and parallel to the Helmholtz field. For the parallel case, the system is approximately described by the differential equation

$$I\ddot{\theta} = -\mu B_s \sin\theta - \eta\dot{\theta} + \mu B_h \sin\theta \sin\omega t, \qquad (1)$$

where θ, labeled in Fig. 1, is the angle between the magnet and the magnetic field produced by the solenoid, B_s is the strength of the solenoid's magnetic field at the position of the magnet, B_h is the amplitude of the oscillating magnetic field due to the Helmholtz coils, μ is the magnitude of the magnetic moment of the magnet, I is the moment of inertia of the magnet, and η is a damping coefficient. Fins made from tape are attached to the magnet to regulate damping. B_s is proportional to the measured solenoid current and B_h is proportional to the measured Helmholtz voltage. The magnet is aligned such that the horizontal component of the Earth's magnetic field is along its axis of rotation.

When the solenoid field is perpendicular to the Helmholtz field, the system is approximately described by

$$I\ddot{\theta} = -\mu B_s \sin\theta - \eta\dot{\theta} + \mu B_h \cos\theta \sin\omega t, \qquad (2)$$

where the parameters are the same as in Eq. (1).

The expected response of the system can be determined by computational techniques. By plotting the time evolution of θ and $\dot{\theta}$ in phase space, a Poincaré map can be used to determine the periodicity and other properties of the system. Analysis of Eq. (2) for B_s equal to zero is discussed in Refs. 3–5. We find similar theoretical results for nonvanishing B_s. Equation (1) also describes a mechanical pendulum driven in the vertical direction.[6] This example is frequently discussed in textbooks on nonlinear systems.[1] In the magnet experiment described here, the "gravity" can be controlled by varying B_s.

Out of the many experiments that can be done with this simple system, we discuss here four applications: the stability of the system, the period-doubling route to chaos, the transient behavior of the system, and higher-order periodicities. In this article, we will focus on the transient behavior, since the other applications have been discussed in Refs. 3–5. For all the discussions that follow, the experimental parameters were adjusted so as to cause the magnet to undergo rotational motion in one direction. The only time the magnet changed its direction of rotation was when

the system went chaotic [see Fig. 3(d)]. The stability of the system is demonstrated in Fig. 2(a), which is the computer graphics output for a Helmholtz voltage of 6 V and a small constant vertical magnetic field. The y axis is the time in seconds that the photogate is blocked, and the x axis records successive rotations. Up to 200 data points, each corresponding to a full rotation of the magnet, can be recorded. As mentioned before, we recorded every other block of the photogate, so the times displayed in all the figures represent the successive blocking times after the magnet has rotated through 360°. Note how low the noise level is; the blocking times vary by about 0.5%. This stability of the output was not achieved until the system was shielded from air currents by a plywood box.

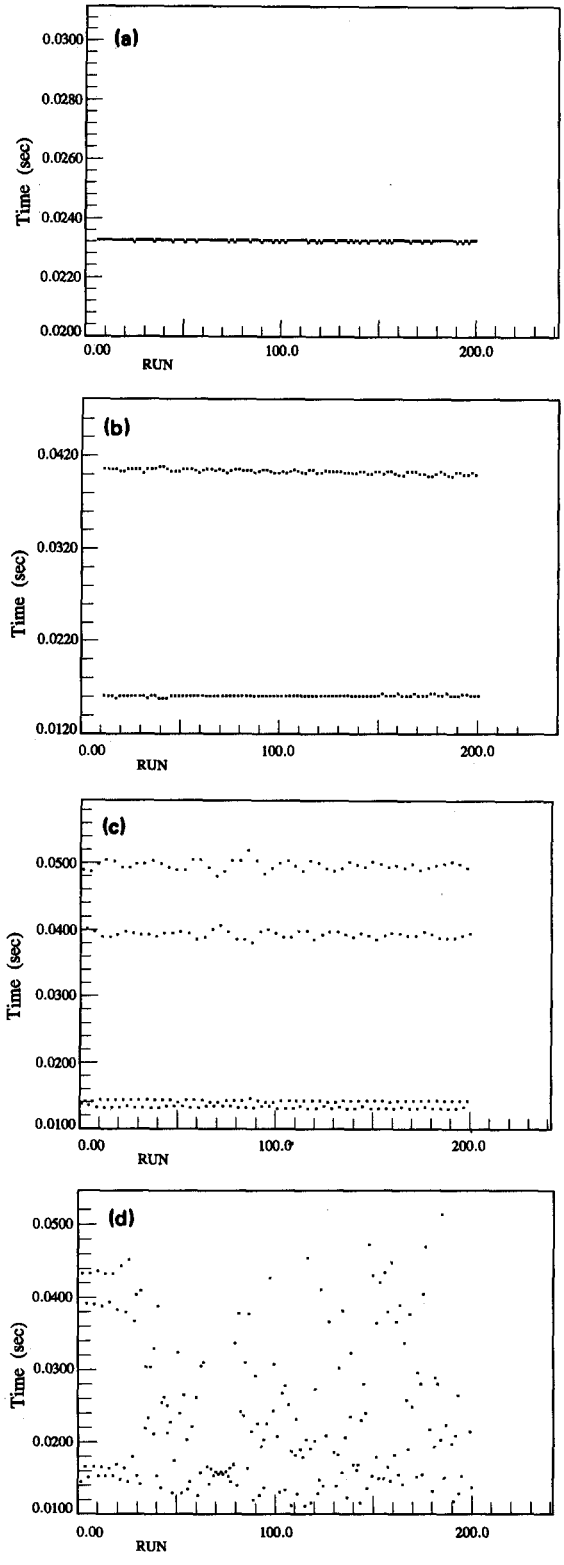

Fig. 2. The period doubling route to chaos is shown in the above sequence of graphs: (a) period 1; (b) period 2; (c) period 4; (d) chaotic motion.

The period-doubling route to chaos can be observed when B_s is parallel to B_h. Results obtained from varying the magnitude of B_h while keeping B_s fixed are shown in Fig. 2(a)–2(d) for relatively light damping. The current through the solenoid is 0.1 A, which produces a magnetic field strength at the position of the magnet of about twice that of the Earth's magnetic field. As the voltage across the Helmholtz coils is increased, the transition from period 1 [Fig. 2(a)] to period 2 [Fig. 2(b)] to period 4 motion [Fig. 2(c)] is observed. In Fig. 2(d), the data were taken while B_h was increased from a value that produced period 4 motion to one that caused chaotic behavior. During this chaotic motion, the magnet randomly changed direction and no periodic behavior was observed over long periods of time (>45 min). A plot of t_{n+1} vs t_n would be useful in plotting strange attractors, however, an ambiguity exists in the blocking time data for this chaotic motion: It is difficult to determine which side of the magnet blocked the photogate, as well as the sign of $\dot{\theta}$ as the magnet spins wildly in both directions. The case of strange attractors for the rotating magnet system is discussed in Ref. 5. Starting again from a stable period 4 motion, a careful increase of B_s led to a period 8 motion, which was not stable due to fluctuations in the electric circuitry. This period 8 motion only lasted for 10 cycles, i.e., 80 revolutions. The period-doubling constant for these first few bifurcations was dependent on the damping and varied from approximately 5 for heavy damping to about 8 for light damping.

Using the photogate to take data, the transient motion of the system as it returns to steady state can be recorded, as shown in Fig. 3(a)–3(d). For these data, the magnet was initially spinning in a stable mode. Then, a strong horseshoe magnet was quickly brought near and quickly removed from the vicinity of the spinning magnet. The time of this magnetic perturbation was less than a second, i.e., less than one rotation of the motion. Figure 3(a)–3(d) show data, for various degrees of damping, in which modes of periods 1 and 2 have been perturbed. The different dampings were obtained by using larger or smaller fins of tape.

The decay parameters of the transient motion can be easily determined from the photogate data. The relevant parameters are derived from the linearization of the map at the point of stability. Mathematical details are discussed in Ref. 7, so we mention here only the points important to our experiment. The spinning magnet has 3 degrees of freedom: the angle θ, the angular velocity $\dot{\theta}$, and the phase of the driving force Δ. Data taken at a fixed angle yield a two-dimensional Poincaré map of the motion, the two dimensions being $\dot{\theta}$ and Δ. Since in this experiment we are not measuring the phase of the driving force simultaneously with $\dot{\theta}$, only a projection of the two-dimensional Poincaré map along the $\dot{\theta}$ axis is recorded. Collecting data via an analog-to-digital card would enable a measurement of the complete two-dimensional Poincaré section.

The transient behavior of the system depends on the eigenvalues of the Jacobian of the map at the stable point, and, consequently, a measurement of these eigenvalues gives insight into the bifurcation scheme of the motion. For

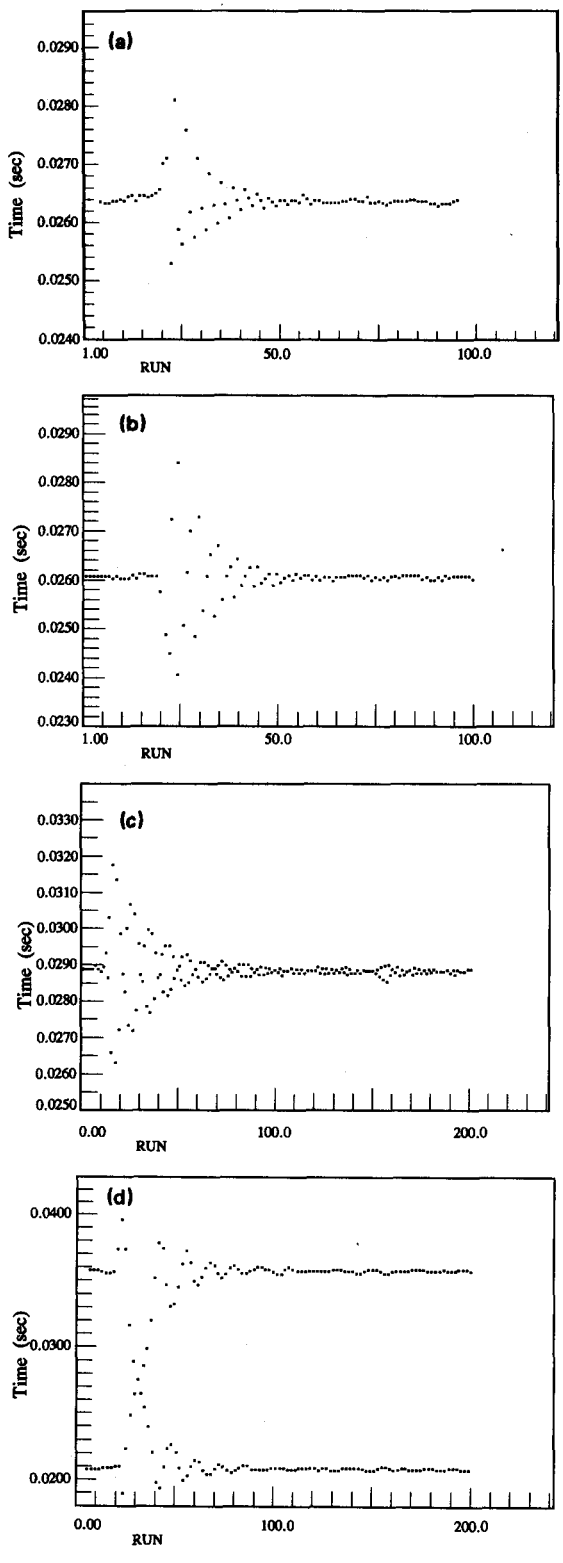

Fig. 3. These graphs demonstrate how transient motion can be analyzed. The system is perturbed, and its return to steady state is recorded: (a) $\alpha = 120°$; (b) $\alpha = 144°$; (c) $\alpha \approx 165°$; (d) $\alpha \approx 55°$. The angle α is defined in the text.

a two-dimensional map, there are two eigenvalues. In particular, for the spinning magnet system with moderate damping the two eigenvalues are complex conjugates of each other, labeled $a \exp(\pm i\alpha)$. If a stable system is perturbed, a plot in the two dimensional $\dot{\theta} - \Delta$ space will be a locus of points which converges to the stable point. For

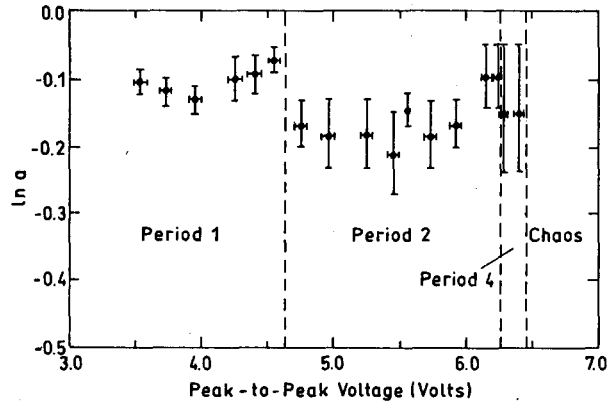

Fig 4. A graph of the experimentally determined damping parameter ln a as a function of the peak-to-peak voltage across the Helmholtz coils is shown.

complex eigenvalues, this locus is a spiral,[7] thus the projection on the θ axis will be

$$\dot{\theta}_n = \dot{\theta}_s + Ke^{n \ln a} \cos(n\alpha + \delta), \tag{3}$$

where $\dot{\theta}_s$ is the steady-state value of the angular velocity and n is the iteration or rotation number, i.e., is the nth rotation of the magnet after the perturbation is applied. The constant K is the initial deviation from $\dot{\theta}_s$, i.e., the magnitude of the initial perturbation. The angle δ is just a relative phase depending on when the perturbation was applied. The experimental data are accurately described by Eq. (3): The transients are exponentially damped sinusoidal functions. Therefore, the parameters a and α can be extracted from the photogate data. For period 2 (or 4, etc.) motion, Eq. (3) will apply to each "branch" of the data.

Measurements were done for a variety of setups, and we display in Figs. 4 and 5 the results for a particular scenario of the period-doubling route to chaos. The data in these figures were obtained for parallel B_s and B_h by varying the magnitude of B_h while keeping B_s fixed. The peak-to-peak voltage was varied, and the parameters ln a and α were measured as the system went through period 1, period 2, period 4 to chaotic motion. As can be seen from Figs. 4 and 5, the most significant variation is in the angle α, which varies from 0–180° in each region of periodicity.

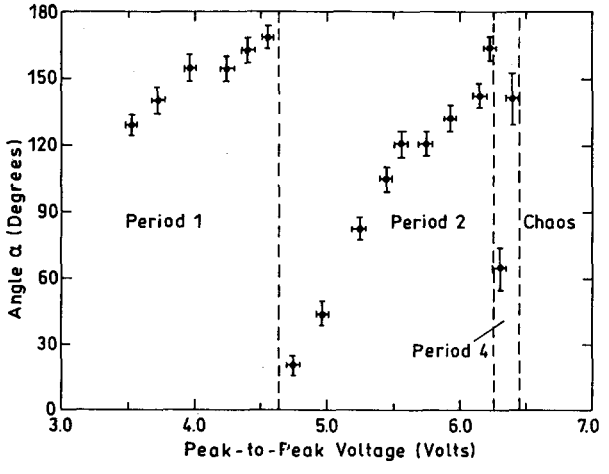

Fig. 5. A graph of the experimentally determined damping parameter α as a function of the peak-to-peak voltage across the Helmholtz coils is shown.

The angle α is determined by dividing 360° by the number of data points per cycle of the sinusoidal decaying motion. For example, consider the graphs of Fig. 3. In Fig. 3(d), α is approximately 55° because the magnet undergoes 13 rotations over two sinusoidal cycles of the transient motion: $\alpha = 360/(13/2)$. In Fig. 3(a), α is 120°, since the decay pattern repeats after exactly three revolutions. An example of α equal to $360/(2.5)$ or 144° is shown in Fig. 3(b). In Fig. 3(c), α is approximately 165°, and a small increase in the driving voltage will cause a bifurcation. The determination of the parameter α is quite suitable for an undergraduate laboratory since it is so easily extracted from the data. One could also define a "transient winding number" N_t equal to $\alpha/180$. This would be the fraction of a semicircle that the Poincaré map winds around as it spirals toward the stable point. N_t varies from zero to one as the system goes between bifurcation values.

The experimental values of ln a plotted in Fig. 4 were obtained from the blocking time data t_n by calculating $1/t_n$, which is proportional to $\dot{\theta}$ in Eq. (3). A plot of $1/t_n$ vs n is an exponentially damped sinusoidal function which approaches a steady-state value of $1/t_s$ at large n,

$$1/t_n = 1/t_s + A_n, \tag{4}$$

where the amplitude A_n is proportional to $e^{n \ln a} \cos(n\alpha + \delta)$ from Eq. (3). A_n has extremities when $\cos(n\alpha + \delta)$ is equal to plus or minus one in this equation. These extreme values of A_n were plotted as a function of n on semilog paper. The slope of a best-fit line was used to determine the value of ln a. In a student laboratory, ln a can be estimated directly from the blocking time data by counting how many rotations it takes for the perturbation to settle down to $1/e$ of its value. For example, in Fig. 3(a) it takes about nine rotations for the deviations from steady state to drop a factor of $\approx 1/e$. Thus ln a is approximately $-1/9$ or -0.11. If the perturbations are too small, ln a is difficult to measure. The quantity ln a is strongly dependent on the amount of damping.

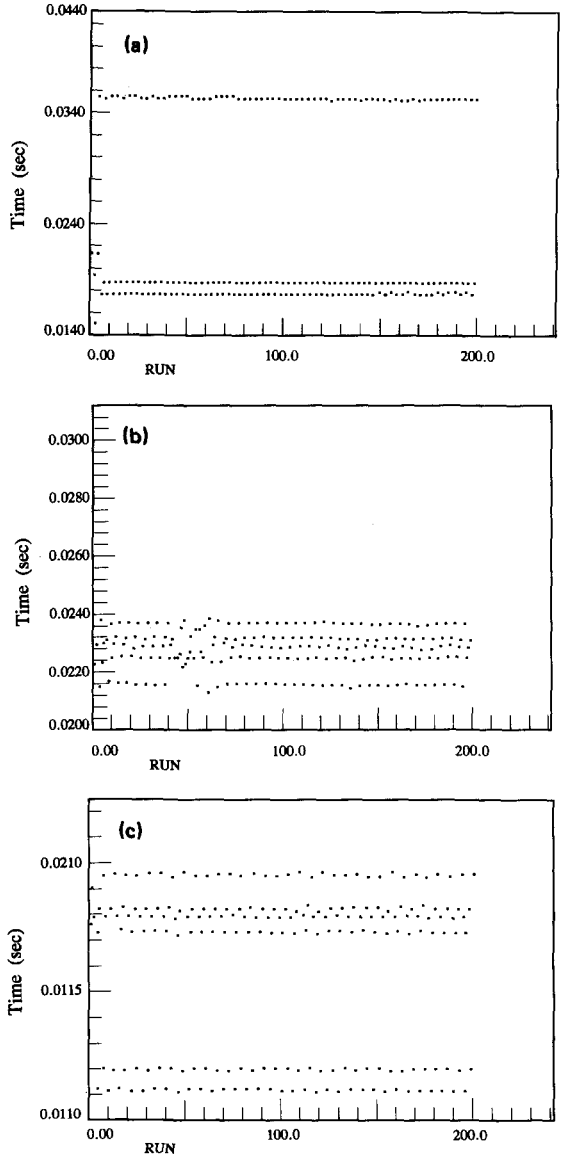

Fig. 6. Other interesting periodic behavior that was observed: (a) period 3 motion; (b) period 5 motion; (c) period 6 motion.

Finally, we mention some interesting motions that did not follow the period-doubling route to chaos. These were obtained when B_s was perpendicular to B_h and, also, when B_s was small and parallel to B_h. We observed the following scenarios: periods 1 to 2 to 6 to chaos; upon lowering B_h we observed periods 2 to 5 to 3 to 1. The data from some of these motions are displayed in Fig. 6(a)–6(c). All of these modes lasted for over 45 mins, they were stable to small perturbations, and persisted until we became tired of watching the magnet and changed B_h. Two different period 6 motions were observed: one in which the magnet rotated in the same direction and another one in which the magnet alternated $2\frac{1}{2}$ times clockwise rotation then $2\frac{1}{2}$ times counterclockwise rotation. A period 7 motion was also observed, but it only lasted around 50 revolutions of the magnet. Measurements of the parameters a and α described above can give insight into the generation of these periodicities and mode lockings.

As a final note, we mention that in order to obtain very stable motion, it is necessary to eliminate all sources of noise. These include air currents and people moving about the room. In addition, the magnetic moment of the magnet may change slightly over a period of hours. Since nonlinear systems can be very sensitive to changes in the parameters, it is important to consider this possible variation.

IV. CONCLUSION

In conclusion, we have pointed out some of the experiments on nonlinear systems that can be done with the simple spinning magnet experiment described above. The period-doubling route to chaos and other periodic behavior is quite easily observed. The use of a photogate to determine blocking times of the magnet at a fixed angle allows an accurate measurement of the time evolution of the system, thus providing a convenient way to observe how the magnet returns to steady state after it has been perturbed. From the experimental data, the real and complex eigenvalues of the Jacobian of the nonlinear map can be measured. Since the experiment can be assembled with common laboratory equipment, it is particularly suited to introduce many properties of nonlinear systems to undergraduate students. As of this writing, two local high schools have set up working systems using their own equipment.

ACKNOWLEDGMENTS

We would like to thank the students in the second-year physics laboratory class for all the analyses and data taking

that they did on this experiment last quarter. We would also like to thank Erik Swenson for his much appreciated help with graphing.

[1]H. Gould and J. Tobochnik, *Computer Simulations Methods* (Addison-Wesley, Reading, MA, 1988).
[2]K. Briggs, "Simple experiments in chaotic dynamics," Am. J. Phys. **55**, 1083–1089 (1987).
[3]V. Croquette and C. Poitou, "Cascade of period doubling bifurcations and large stochasticity in the motions of a compass," J. Phys. Lett. **42**, 537–539 (1981).
[4]H. Meissner and G. Schmidt, "A simple experiment for studying the transition from order to chaos," Am. J. Phys. **54**, 800–804 (1986).
[5]M. J. Ballico, M. L. Sawley, and F. Skiff, "The bipolar motor: A simple demonstration of deterministic chaos," Am. J. Phys. **58**, 58–61 (1990).
[6]J. B. McLaughlin, "Period-doubling bifurcations and chaotic motion for a parametrically forced pendulum," J. Stat. Phys. **24**, 375 (1981).
[7]S. Neil Rasband, *Chaotic Dynamics of Nonlinear Systems* (Wiley, New York, 1990), pp. 135–138.

The route to chaos in a dripping water faucet[a)]

K. Dreyer and F. R. Hickey
Department of Physics, Hartwick College, Oneonta, New York 13820

(Received 16 July 1990; accepted for publication 10 October 1990)

The dripping water faucet is a simple system which is shown in this article to be rich in examples of chaotic behavior. Data were taken for a wide range of drip rates for two different faucet nozzles and plotted as discrete time maps. Different routes to chaos, bifurcation and intermittency, are demonstrated for the different nozzles. Examples of period-1, -2, -3, and -4 attractors, as well as strange attractors, are presented and correlated to the formation of drops leaving the faucet.

I. INTRODUCTION

During the past decade, there has been increasing interest in dynamic systems which exhibit chaotic behavior. The term "chaotic" is generally used to describe nonlinear, but deterministic systems whose dynamic behavior proceeds from stable points through a series of stable cycles to a state where there is no discernible regularity or order. A permanent magnet in an oscillating magnetic field,[1] a bounding ball,[2,3] an inverted pendulum,[4] and a bipolar motor[5] represent some of the mechanical systems which exhibit this behavior.

In 1977, Rossler[6] suggested that a dripping water faucet might exhibit chaotic transition as the flow rate is varied. His prediction was experimentally confirmed a few years later by Shaw.[7] Since then, the nonlinear behavior of a dripping faucet during the transition to chaos has been examined by several authors.[8–12]

One way to study the dynamics of a dripping faucet is to measure the time interval t_N between successive drops. The time series thus obtained can then be plotted in a time-delay coordinate system (t_{N+1} vs t_N) to obtain a two-dimension-

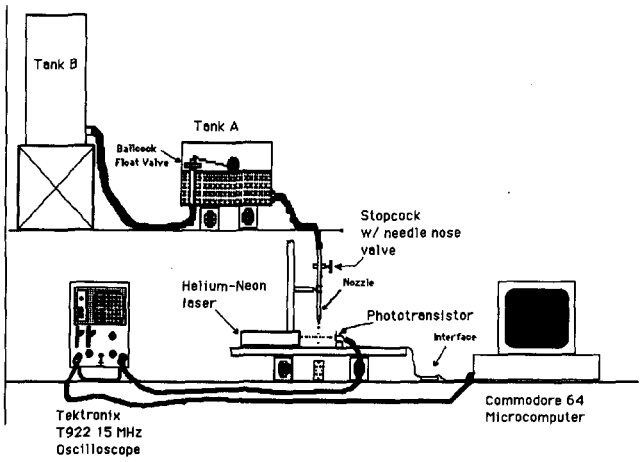

Fig. 1. Block diagram of apparatus used to measure drip rates.

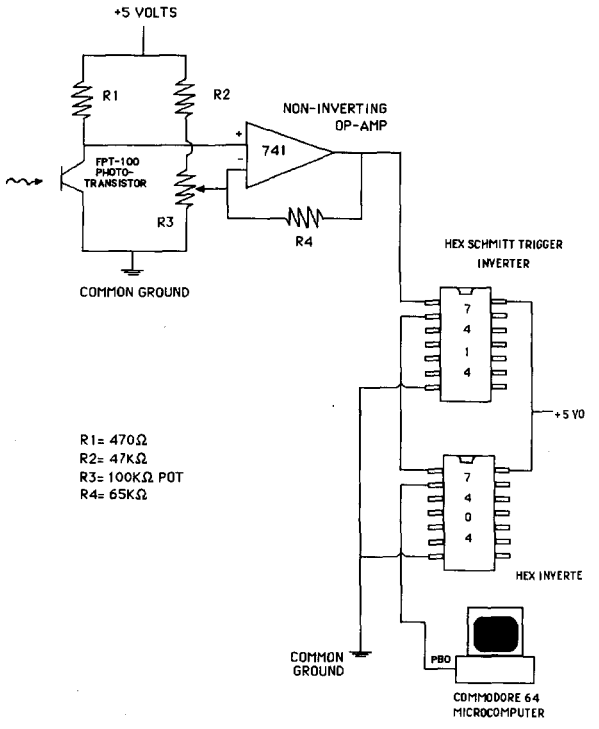

Fig. 2. Circuit used to amplify and shape signals generated by the photo-transistor.